CHITOSAN AEROGEL BEADS WITH MICROFIBRILLATED CELLULOSE SKELETON FOR REMOVAL OF FORMALDEHYDE FROM INDOOR AIR

PENG WU and ZHIMING LIU

College of Material Science and Engineering, Northeast Forestry University, 26, Hexing Road, Harbin 150040, Heilongjiang, People's Republic of China
✉ *Corresponding author: Zhiming Liu, zhimingliu@nefu.edu.cn*

Received September 1, 2015

Formaldehyde is present to some degree in indoor air, and poses a considerable threat to human health. The development of efficient and effective sorbent materials is highly necessary, in order to remove formaldehyde and better safeguard the health of a building's occupants. This study explores a new chitosan aerogel bead supported by microfibrillated cellulose, found to be an efficient biosorbent for formaldehyde, with high sorption capacity. Adsorption tests demonstrate that the sample prepared at a chitosan/MFC weight ratio of R=1 exhibits the highest specific surface area (1351 m^2/g) and maximum HCHO adsorption capacity (2.2 $mmol_{HCHO}\ g^{-1}$). The outstanding sorption performance of the aerogel beads is associated with their unique physical and chemical properties, including low density, high porosity and specific surface area, as well as abundant surface-activated amino groups. This study provides valuable information for the fabrication of novel, environmentally friendly aerogel beads with high HCHO adsorption performance for indoor air purification.

Keywords: chitosan aerogel beads, formaldehyde cleaning, microfibrillated cellulose

INTRODUCTION

Formaldehyde, which at room temperature is a colorless, characteristically pungent, irritating gas, is a rather common indoor pollutant that is emitted from indoor furniture paint, flooring materials, wallpaper, and cigarette smoke.[1,2] At concentrations above 0.1 ppm in an indoor environment, formaldehyde has been shown to cause a series of health problems related to "Sick Building Syndrome" (SBS).[3] Recent studies have also shown a positive correlation between exposure to formaldehyde and the development of leukemia, particularly myeloid leukemia.[4,5] To this effect, emitted formaldehyde gas in indoor air is extremely harmful and its removal is a crucial consideration.

Various technologies have been developed for the purpose of removing formaldehyde from indoor environments, including adsorption,[6-9] catalytic oxidization,[10,11] and botanical filtrations.[12] Considering the costs and convenience, the adsorption method is a favorable method for pollutant treatment and environmental purification. The adsorptive removal of volatile aldehydes focuses on amine-functionalized materials, effective due to utilization of azomethine or Schiff bases between aldehydes and targeted materials.[13,14] When a Schiff base is formed, however, the adsorbed formaldehyde is not released from the adsorbent even heated to 60 °C for 2 h.[15] Additionally, synthetic amine-functionalized materials are generally rather expensive and may cause secondary pollution of the environment when they are discarded. Chitosan, a renewable and biodegradable amino polysaccharide obtained from chitin after deacetylation, is already widely used as water treatment material,[16-19] and has been shown to absorb gaseous aldehydes such as formaldehyde and acetaldehyde as well.[20] The efficiency of formaldehyde adsorption of the traditional form of chitosan, however, is not very high,[21,22] which calls for expanding its specific surface area and increasing its number of active amine to improve its adsorption efficiency.

Aerogels are a class of low-density solids that possess open three-dimensional mesoporous structure and high specific surface area, and thus show potential application as adsorbents, thermal insulators, acoustic absorbers, catalysts, and catalyst supports.[23-25] Biomass aerogel materials possess features of traditional aerogels, plus certain additional advantages, such as renewability, abundant availability, low cost, and environmental friendliness.[26,27] Their chitosan backbone, however, is highly polar and forms strong hydrogen bonds between adjacent chains – thus it does not easily maintain a high specific surface area due to severe shrinkage and deformation of the gel.[20] In an effort to remedy

this, previous studies investigated cross-linked and blended chitosan with organic and/or inorganic compounds to successfully improve the specific surface area of the chitosan aerogel.[28,29] The present study utilizes environmentally friendly and highly strong microfibrillated cellulose (MFC) as skeleton for surface tethering of chitosan molecules, and demonstrates that chitosan aerogel containing MFC is an excellent candidate material for gaseous formaldehyde removal. Moreover, the spherical aerogel can be quite easily incorporated into air purification systems or filters to improve overall air quality.

EXPERIMENTAL

Materials

Commercial chitosan was purchased from Sigma-Aldrich, with a viscosity of 55 mPas and deacetylation degree of over 96 wt%. *Phyllostachys heterocycla cv. pubescens* bamboo was obtained from Huang-gongwang Forest Park in Fuyang, Zhejiang Province, China, and dried, ground and screened to obtain 60-80 mesh particle size bamboo powder. All other chemicals were of analytical grade and used without further purification.

Investigation methods

Synthesis of aerogel beads

Bamboo powder was purified by a series of chemical treatments, as described by Okahisa[30] and Abe.[31] Microfibrillated cellulose (MFC) was fabricated by the homogenization process.[32,33] First, the extractives of bamboo powder were removed using an ethanol-toluene solution for 6 h in the Soxhlet apparatus. Afterwards, any lignin in the sample was removed by an acidified sodium chlorite solution at 70 ºC for 5 h. Next, hemicellulose in the sample was treated in 5 w% potassium hydroxide aqueous solution at room temperature for 24 h. Lastly, the sample was filtered and rinsed with distilled water until the residue was neutralized. After the purification process, the as-purified cellulose was dispersed in 300 ml deionized water and homogenized using a high-pressure fluidizer (Microfluidizer M-110, Microfluidics Corp., USA) equipped with 87 μm-sized chambers. Full homogenization was achieved after 12 cycles at an operating pressure of 20,000 psi. Finally, the MFC hydrosol was obtained and diluted to approximately 1 wt%.

Aerogel beads were synthesized using the hand-dropping procedure, based on the pH inversion.[34,35] For the synthesis of spherical aerogels at the chitosan/MFC weight ratio R=1, 1 g chitosan was initially dissolved in 2% v/v aqueous solution (100 mL) of acetic acid, followed by mixing the above solution of MFC hydrosol (100 mL) with ultrasonic dispersion for 20 min. The mixture with the pH value of 3.97 and viscosity of 42.6 mPa·s was then dropped into 2 L of 0.1mol/L NaOH solution with a 1 mL disposable plastic pipette, and solidified at room temperature for 12 h before rinsing under running deionized water for 12 h. To prevent the hydrogel networks from collapsing during the drying process, the obtained hydrogel samples were first exchanged with ethanol, then with *t*-butyl alcohol, with several exchanges in each solvent sample. The *t*-butyl alcohol-included gel was subjected to freeze drying. The samples were also prepared at R = 0 (without chitosan), 3 (chitosan/MFC weight ratio), and ∞ (without cellulose) under the same conditions described above. The samples prepared at R = 0, 1, 3, and ∞ were labeled CAB-0, CAB-1, CAB-3, and CAB-∞, respectively. For different acidity to different proportions of the mixture during synthesis of the gel beads, there is little impact on the pH within excessive sodium hydroxide coagulating bath.

Characterization of aerogel beads

The surface morphology of the aerogel samples was analyzed with a scanning electron microscope (SEM, FEI QUATA200). The beads were coated with gold for observation and photographed at an accelerating voltage of 12.5 kV.

The Brunauer-Emmett-Teller (BET) specific surface areas and porous structures of the samples were characterized using a Micromeritics ASAP 2020 nitrogen adsorption apparatus (USA). All samples were degassed at 120 ºC before nitrogen adsorption measurements.

The Fourier transform infrared (FT-IR) spectra were acquired with a Specttwn 2000 instrument (Perkin Elmer, USA) using a diamond single reflection attenuated total reflectance (FTIR-ATR) device. Duplicate spectra per sample were obtained with 32 scans per spectrum at a spectral resolution of 4 cm^{-1} in a wavenumber range from 4000 to 650 cm^{-1}.

X-ray photoelectron spectroscopy (XPS) measurement was performed using a Model PHI-5700 ESCA apparatus (Physical Electronics, USA). A monochromatic Al Kα (1,486.6 eV) X-ray source and 40 eV pass energy of analyzer were used under ultra-high vacuum conditions (5.2×10^{-9} Torr). All binding energies (BE) were referenced with adventitious carbon (binding energy = 284.6 eV).

Formaldehyde adsorption experiments

The aerogel beads were tested for adsorption performance in a self-designed sealed amber chamber at room temperature, as shown in Figure 1, where the total volume of chamber was approximately 5 L. Before formaldehyde abatement tests, all adsorbent samples were dried under vacuum (ca. 200 Pa) overnight at ca.

100 °C to remove physisorbed moisture and impurities, then the prepared samples (10 mg) were wrapped in qualitative filter paper (pore size and diameter of 15-20 μm and 15 cm, respectively) and hung in the chamber. In order to ensure complete formaldehyde gasification, the chamber was first fully evacuated, then injected with 8 μL of aqueous formaldehyde solution (10 wt%) by a microsyringe. N_2 gas was also introduced in order to maintain atmospheric pressure.

Then, the system was equilibrated over time at room temperature. Formaldehyde gas concentrations were determined using the HPLC method.[36] 3.0 g/L 2,4-dinitrobenzene in acetonitrile solution (2 mL), and 2 mL acetonitrile were added into the absorption tube, while H_2 was continually fed into the chamber in order to make the residual formaldehyde in the chamber completely pass the 2,4-dinitrophenylhydrazine (DNPH) sorbent and form a DNPH-formaldehyde adduct. The extract was analyzed using an HPLC system from Shimadzu, which consisted of C18 chemical-bonded silica gel columns as a partitioner phase, a mobile phase of acetonitrile and water (60:40 v/v) at a flow rate of 1 mL/min at 40 °C, and a UV detector at 360 nm. The formaldehyde gas concentration inside the container was determined by calibrating the peak area with formaldehyde standard solutions.[13] The adsorption quantities of samples at 30, 60, 120, 180, and 300 min were measured three times according to the above method.

RESULTS AND DISCUSSION

Characterization of materials

SEM analysis

The aerogel beads obtained from the corresponding hydrogel samples with a chitosan/MFC weight ratio of R=0 to ∞ after freeze-drying have been assessed as successfully prepared. As shown in Figure 2, all samples are spherical or ellipsoidal and form similar three-dimensional network structures with micro and mesopores. The cellulose aerogel beads (CAB-0), however, show small volume shrinkage change during the gelation and drying process; their network is formed by the aggregation and winding of individual microfibrillated cellulose, which is very similar to those isolated from plant material, as indicated in a previous study.[37] Conversely, for the pure chitosan samples (CAB-∞), partial fibers seem to have thickened, and their network has become more intensive and non-uniform – likely due to the high polarity of chitosan molecules and the formation of strong hydrogen bonds between adjacent chains.[20] As for the composite samples, results show that higher MFC concentration lessened the volume shrinkage of the beads, attributed to the skeletal reinforcement of MFC in the chitosan aerogel system.

BET analysis

The N_2 adsorption/desorption isotherms and pore-size distribution curves, as shown in Figure 3, also demonstrate that isotherms exhibit type IV characteristics with a pronounced type H1 hysteresis loop, typical of mesoporous materials, according to IUPAC.[38] Further, the exploding sorption capacity within a relatively high P/P_0 range reflects the presence of excessive large-diameter mesoporosity and macroporosity of inter-fibril voids,[30] which can be expected from CAB-0 with 98.4 vol% overall porosity (calculated from apparent density and true density of cellulose). Among these isotherms, the CAB-1 shows the highest adsorption volume, implying that the introduction of MFC into chitosan aerogel does not change the essential microstructural characteristics of chitosan aerogel beads, but only affects the surface area and pore space available for N_2 adsorption, while reducing the aggregation of chitosan molecular adjacent chains.

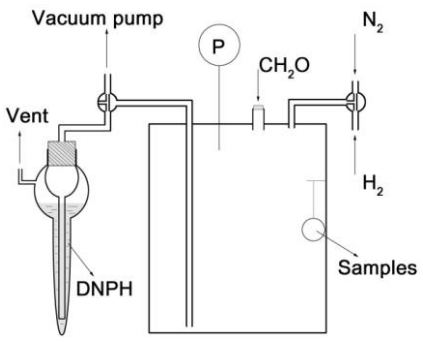

Figure 1: Experimental apparatus for the formaldehyde adsorption test

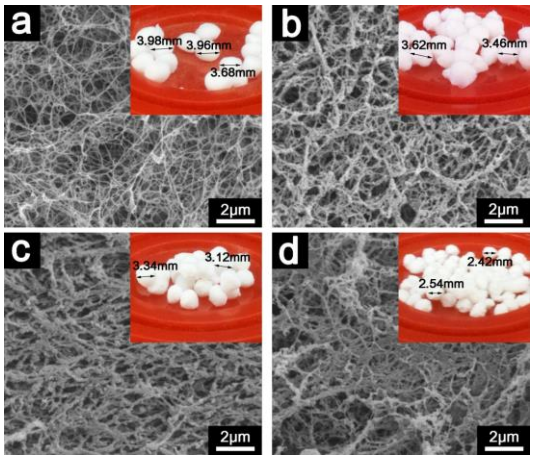

Figure 2: SEM images and photographs of composite aerogel beads with different chitosan/MFC weight ratio of (a) CAB-0, (b) CAB-1, (c) CAB-3, and (d) CAB-∞ (Insets show photographs of corresponding samples)

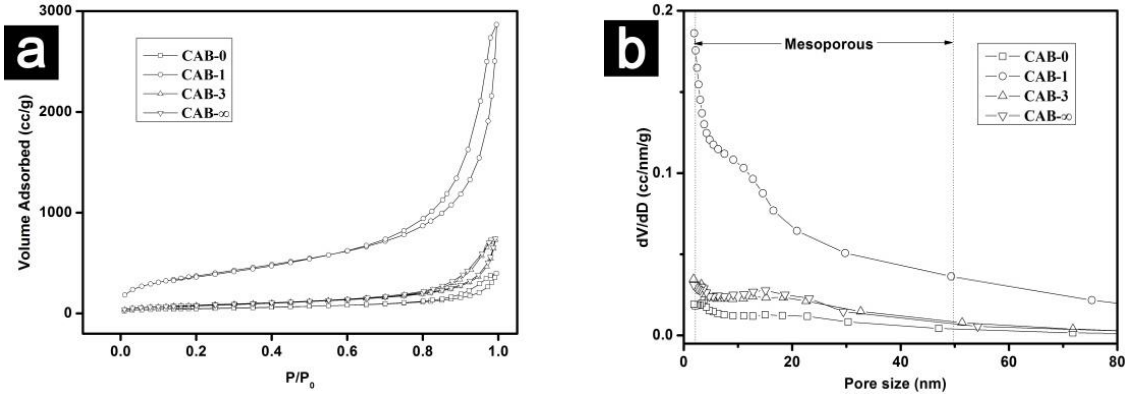

Figure 3: Nitrogen adsorption-desorption isotherms (a) and corresponding pore size distribution curves (b) of CAB-0, CAB-1, CAB-3 and CAB-∞ samples

Table 1
Porosity characteristics of composite aerogel beads with different chitosan/MFC weight ratios

Sample	Apparent density, mg/cm^3	S_{BET} (from micropores), m^2/g	Pore volumes (from micropores), cm^3/g	Average pore size, nm
CAB-0	19.2±0.6	173 (12)	0.619 (0.005)	12.96
CAB-1	26.1±0.4	1351 (110)	4.486 (0.053)	12.31
CAB-3	31.0±1.2	291 (22)	1.139 (0.010)	13.37
CAB-∞	59.6±2.1	299 (19)	1.157 (0.009)	13.39

Figure 3(b) displays the corresponding pore size distributions of the samples. All beads exhibit a bi-modal distribution with the first pore size peak located in the micropore region, and the main pore size peak located in the mesopore region. Relevant structural parameters derived from the isotherms are summarized in Table 1. The CAB-1 sample shows the largest specific surface area and highest pore volume compared to the other samples. The specific surface area, average pore size, and pore volume of the CAB-1 sample is 1351 m^2/g, 12.31 nm, and 4.486 cm^3/g, respectively. The mesopores in CAB-1 contribute 91.8% (1241 m^2/g) of the specific surface area and 98.8% (4.433 cm^3/g) of the pore volume. This indicates that the mesopores of the CAB-1 samples function quite effectively as gas purifiers.

FTIR analysis

FITR analysis has been also performed in order to investigate possible chemical interaction between MFC and chitosan in the composite aerogel beads (Fig. 4). The FTIR spectra of pure chitosan aerogel (CAB-∞) shows a broad band at 3445 cm^{-1} due to O-H and N-H stretching, whereas the two bands at 1670 and 1600 cm^{-1} are attributed to C=O of amide I and N-H of amide II.[39,40] The FTIR spectrum of MFC aerogel (CAB-0) shows characteristic bands at 3342 cm^{-1} due to O-H stretching

vibration, the peaks at 2900 cm^{-1} for C-H stretching, and the peak at 1630 cm^{-1} associated with the H–O–H stretching vibration of absorbed water in carbohydrates, respectively.[41] All the peaks of CAB-1 are found in the spectrum of CAB-0 (MFC) or CAB-∞ (chitosan) without any changes in peak position, implying that CAB-1 is simply a physical mixture of MFC and chitosan. The results reveal the absence of any chemical interaction between MFC and chitosan besides breakage of hydrogen bonds during the processes of dissolution and regeneration.

XPS analysis

Representative O 1s, N 1s and C 1s peaks of CAB-1 and CAB-∞ are displayed in Figure 5. The C 1s peak shows three components: at 284.8 eV, typical of carbon only bound to carbon and hydrogen [C-(C, H)]; near 286.2 eV, typical of carbon forming a single bond with oxygen or nitrogen [C-(O, N)]; and near 287.7 eV, typical of acetal and amide [O-C-O, N-C=O]. The N 1s contribution near 399.3 eV is due to non-protonated amine or amide.[42] The major O 1s contribution found at 532.7 ± 0.1 eV is due to oxygen in the polysaccharide backbone [O-H], while a small component near 531.0 ± 0.2 eV is attributed to ether groups in the polysaccharide backbone and amide polysaccharide backbone [C-O-C, C=O].[43]

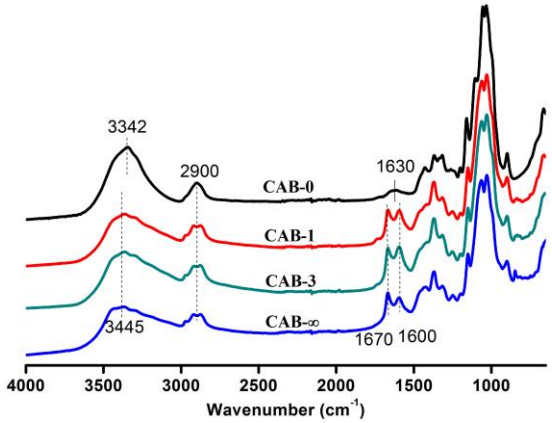

Figure 4: FTIR spectra of composite aerogel beads with different chitosan/MFC weight ratios

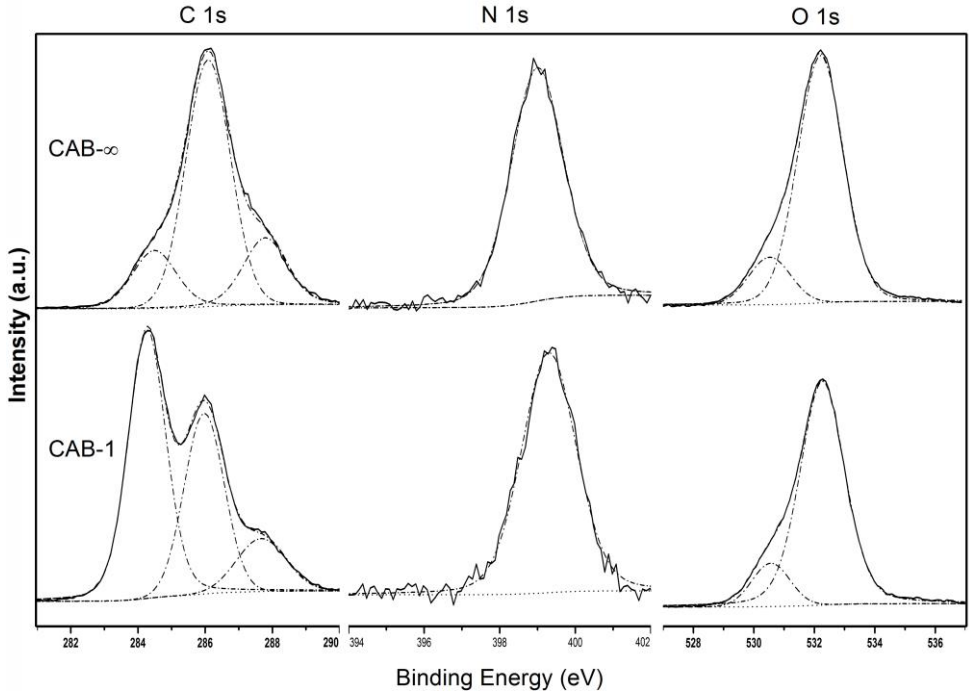

Figure 5: C 1 s, O 1 s and N 1 s XPS regions in the CAB-1 and CAB-∞

Table 2
Elemental surface composition of CAB-1 and CAB-∞

Sample	Atomic surface concentration obtained by XPS (%)		
	C	N	O
CAB-1	54.75	6.84	38.41
CAB-∞	69.38	4.25	26.38

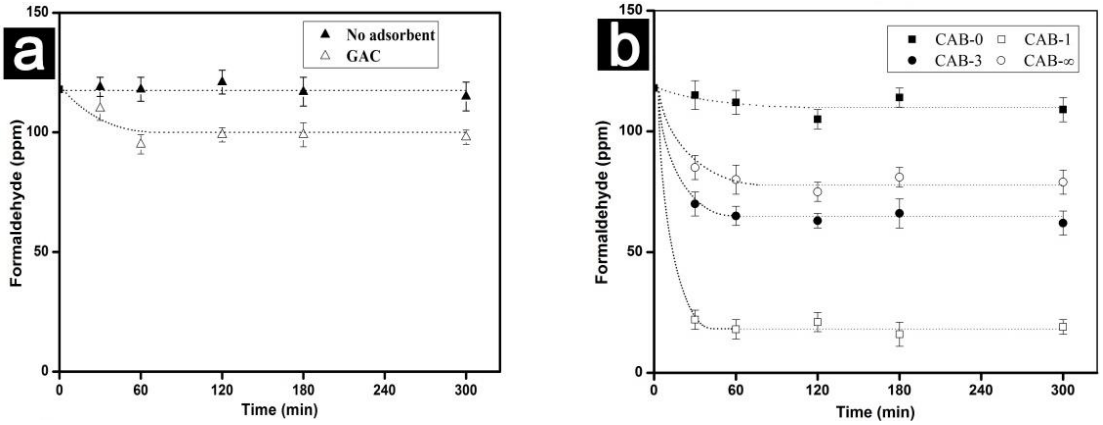

Figure 6: Formaldehyde concentrations inside the gas chamber plotted against time elapsed after its injection

According to these peak areas, the elemental surface compositions are calculated as listed in Table 2. Though the chitosan content of CAB-1 is half that of CAB-∞, CAB-1 shows higher N content than half of CAB-∞, which is indicative of the high mechanical strength of the MFC framework. Chitosan molecules expose more active amino groups to the surface of the aerogel, which is beneficial to formaldehyde gas absorption.

Adsorption performances of formaldehyde

Figure 6(a) and (b) show the results of formaldehyde abatement testing. The gas chamber with no adsorbent maintains the initial formaldehyde concentration (118 ppm), showing that no significant leakage of formaldehyde gas occurred within the examined time period (Fig. 6(a)). In order to demonstrate the adsorption capacity of the pre-prepared samples, the same weight as the test sample of coconut shell activated carbon (GAC, obtained from Beijing Walter Liyuan Environmental Protection Technology Co. Ltd., with specific surface area and pore volume of 590-1500 m^2/g and 0.7-1 cm^3/g, respectively) has been used as control sample under the same conditions. The gas chamber with the GAC adsorbent slightly decreases the formaldehyde concentration to 100 ppm (84.7% of the starting concentration), due to the high surface area of GAC. The CAB-0 also slightly decreases the gas concentration to 110 ppm, (93.2% of its initial concentration), suggesting that formaldehyde is partially adsorbed onto the cellulose surface. The CAB-1 adsorbent dramatically decreases the formaldehyde concentration to 19 ppm (16.1% of the initial concentration) within an hour. This clearly indicates that surface-accessible amine groups play a crucial role in the adsorption of formaldehyde. Compared to CAB-1, both CAB-3 and CAB-∞ adsorb formaldehyde less efficiently, only decreasing formaldehyde concentration to 67 ppm and 77 ppm, respectively. Under the assumption that all removed formaldehyde is tapped into the adsorbent, the adsorption capacity, q, is derived as listed in Table 3. Notably, the q of CAB-1 (2.2 $mmol_{HCHO}$ g^{-1}) is the highest among all the test samples. This supports the theory that CAB-1 is a very successful formaldehyde abatement material.

FTIR analysis, as shown in Figure 7, has been adopted to further investigate formaldehyde adsorption mechanisms of CAB-1. After adsorption, all characteristic bands at 3440 (O-H and N-H stretching), 1670 (C=O of amide I), and 1600 cm^{-1} (N-H of amide II) of CAB-1 are similar to those of CAB-1 without formaldehyde adsorption.

Table 3
Formaldehyde adsorption capacities, q

Sample	q ($mmol_{HCHO}$ g^{-1})
GAC	0.3
CAB-0	0.1
CAB-1	2.2
CAB-3	1.1
CAB-∞	0.9

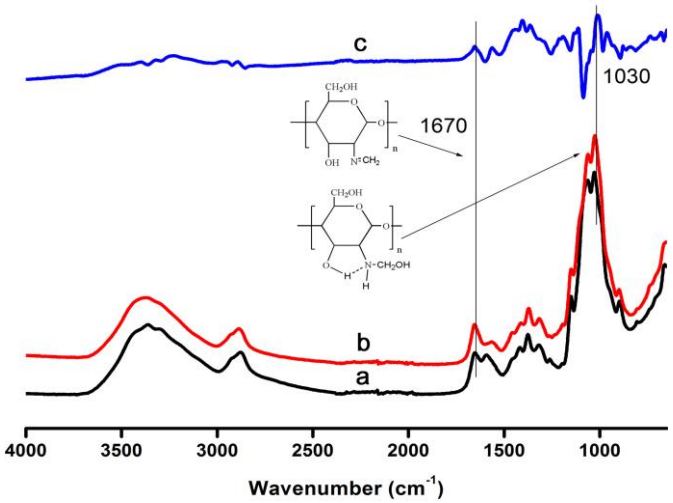

Figure 7: FTIR spectra of CAB-1 after formaldehyde adsorption at 0 (a), and 300 min (b), and a different spectrum of CAB-1 at 300 min adsorption time after subtraction of CAB-1 without adsorption (c)

To better understand the changes of the functional groups, a different FTIR spectrum after a subtraction of CAB-1 without adsorption from the formaldehyde-adsorbed CAB-1 at 300 min is generated, as well. The appearance of a positive band at 1670 cm^{-1} (-C=N of Schiff base) is due to a nucleophilic addition of amines of chitosan to carbonyl of formaldehyde, followed by an elimination of water (H_2O).[39,44] In addition, a sharp, positive, different band at 1030 cm^{-1} (aliphatic C-N), corresponding to carbinolamine intermediate with a very stable five-membered ring due to intra-molecular H-bonding was also observed.[45,46] This demonstrates that formaldehyde gas can be chemically adsorbed by chitosan-based materials via a reaction of primary (1°) amines, which form carbinolamine and Schiff bases.

CONCLUSION

Chitosan aerogel beads with a skeleton of microfibrillated cellulose (MFC) were successfully prepared using the ball dropping method and freeze-drying technique, with MFC and chitosan as raw materials. The sample (CAB-1) prepared at the chitosan/MFC weight ratio R (w/w) =1 contained abundant mesopores. The introduction of MFC exhibits a significant influence on specific surface areas. The CAB-1 sample showed the highest specific surface area (1351 m^2/g) and presented favorable formaldehyde adsorption capacity (2.2 $mmol_{HCHO}$ g^{-1}). This indicates that the amine groups of chitosan, as well as the high specific surface area and porous volume of the samples, are beneficial characteristics to the adsorption of formaldehyde. This study provides a new insight into the design and fabrication of bioadsorbents with high HCHO removal performance for indoor air purification.

ACKNOWLEDGEMENTS: The research was supported by the Fundamental Research Funds for the Central Universities (2572014EB01-02; 2572014AB20). The authors would also like to thank for the financial support provided by the Key Laboratory of Wood Science and Technology, Zhejiang Province (2014lygcz002). Special thanks are given to Prof. Shujun Li for her test equipment and analysis.

REFERENCES

[1] H. B. An, M. J.Yu, J. M. Kim, M. Jin, J. K Jeon *et al*., *Nanoscale Res. Lett*., **7**, 1 (2012).
[2] W. J. Liang, J. Li, J. X. Li, T. Zhu and Y. Q. Jin, *J. Hazard. Mater*., **175**, 1090 (2010).
[3] P. Chin, L. P. Yang and D. F. Ollis, *J. Catal*., **237**, 29 (2006).
[4] V. J. Cogliano, Y. Grosse, R. A. Baan, K. Straif, M. B. Secretan *et al*., *Environ. Health Persp*., **113**, 1205 (2005).
[5] M. Hauptmann, J. H. Lubin, P. A. Stewart, R. B. Hayes and A. Blair, *Am. J. Epidemiol*., **159**, 1117 (2004).
[6] Y. Le, D. P. Guo, B. Cheng and J. G. Yu, *Appl. Surf. Sci*., **274**, 110 (2013).
[7] K. J. Lee, N. Shiratori, G. H. Lee, J. Miyawaki, I. Mochida *et al*., *Carbon*, **48**, 4248 (2010).
[8] Z. H. Xu, J. G. Yu, G. Liu, B. Cheng, P. Zhou *et al*., *Dalton T*., **42**, 10190 (2013).
[9] S. Yamanaka, T. Oiso, Y. Kurahashi, H. Abe, K. Hara *et al*., *J. Nanopart. Res*., **16**, 1 (2014).
[10] C. Y. Ma, D. H. Wang, W. J. Xue, B. J. Dou, H. L. Wang *et al*., *Environ. Sci. Technol*., **45**, 3628 (2011).
[11] C. B. Zhang, H. He and K. Tanaka, *Catal. Commun*., **6**, 211 (2005).
[12] N. Lu, J. J. Pei, Y. X. Zhao, R. Y. Qi and J. J. Liu, *Build. Environ*., **57**, 253 (2012).
[13] A. M. Ewlad-Ahmed, M. A. Morris, S. V. Patwardhan and L. T. Gibson, *Environ. Sci. Technol*., **46**, 13354 (2012).
[14] H. Q. Rong, Z. Y. Liu, Q. L. Wu, D. Pan and J. T. Zheng, *Cellulose*, **17**, 205 (2010).
[15] J. J. Pei and J. S. Zhang, *Chem. Eng. J*., **167**, 59 (2011).
[16] A. I. Cocârta and E. S. Dragan, *Cellulose Chem. Technol*., **48**, 495 (2014).
[17] W. S. Wan Ngah, L. C. Teong and M. A. K. M. Hanafiah, *Carbohyd. Polym*., **83**, 1446 (2011).
[18] A. H. Jawad and M. A. Nawi, *Carbohyd. Polym.*, **90**, 87 (2012).
[19] Y. M. Zhou, S. Y. Fu, L. L. Zhang, H. Y. Zhan and M. V. Levit, *Carbohyd. Polym*., **101**, 75 (2014)
[20] X. H. Chang, D. R. Chen and X. L. Jiao, *J. Phys. Chem. B*, **112**, 7721 (2008).
[21] A. El Kadib and M. Bousmina, *Chem.-Eur. J*., **18**, 8264 (2012).
[22] N. Li and R. B. Bai, *Sep. Purif. Technol*., **42**, 237 (2005).
[23] H. C. Bi, Z. Y. Yin, X. H. Cao, X. Xie, C. L. Tan *et al*., *Adv. Mater*., **25**, 5916 (2013).
[24] K. H. Kim, M. Vural and M. F. Islam, *Adv. Mater*., **23**, 2865 (2011).
[25] J. T. Korhonen, M. Kettunen, R. H. A. Ras and O. Ikkala, *ACS Appl. Mater. Inter*., **3**, 1813 (2011).
[26] J. Li, Y. Lu, D. J. Yang, Q. F. Sun, Y. X. Liu *et al*., *Biomacromolecules*, **12**, 1860 (2011).
[27] Y. Lu, Q. F. Sun, D. J. Yang, X. L. She, X. D. Yao *et al*., *J. Mater. Chem.*, **22**, 13548 (2012).
[28] S. Nuasaen, P. Opaprakasit and P. Tangboriboonrat, *Carbohyd. Polym*., **101**, 179 (2014).
[29] K. H. Yang, Y. C. Liu, C. C. Yu and B. C. Chen, *Mater. Chem. Phys*., **126**, 993 (2011).
[30] Y. Okahisa, A. Yoshida, S. Miyaguchi and H. Yano, *Compos. Sci. Technol*., **69**, 1958 (2009)
[31] K. Abe and H. Yano, *Carbohyd. Polym*., **85**, 733 (2011).
[32] M. Henriksson, L. A. Berglund, P. Isaksson, T. Lindstrom and T. Nishino, *Biomacromolecules*, **9**, 1579 (2008).
[33] S. Y. Lee, S. J. Chun, I. A. Kang and J. Y. Park, *J. Ind. Eng. Chem*., **15**, 50 (2009).
[34] A. El Kadib, K. Molvinger, T. Cacciaguerra, M. Bousmina and D. Brunel, *Micropor. Mesopor. Mat*., **142**, 301 (2011).
[35] M. Gericke, J. Trygg and P. Fardim, *Chem. Rev*., **113**, 4812 (2013).
[36] A. Nomura and C. W. Jones, *ACS Appl. Mater. Inter*., **5**, 5569 (2013).
[37] K. Abe and H. Yano, *Cellulose*, **17**, 271 (2010).
[38] H. C. Chien, W. Y. Cheng, Y. H. Wang and S. Y. Lu, *Adv. Funct. Mater*., **22**, 5038 (2012).
[39] G. H. He, Z. Wang, H. Zheng, Y. H. Yin, X. Xiong *et al*., *Carbohyd. Polym*., **90**, 1614 (2012).
[40] M. L. Li, J. Xu, R. H. Li, D. G. Wang, T. B. Li *et al*., *J. Colloid Interf. Sci*., **417**, 131 (2014).
[41] W. S. Chen, H. P. Yu and Y. X. Liu, *Carbohyd. Polym*., **86**, 453 (2011).
[42] P. H. F. Pereira, H. J. C. Voorwald, M. O. H. Cioffi, M. L. C. P. Da Silva, A. M. B. Rego *et al*., *Cellulose*, **21**, 641 (2014).
[43] I. F. Amaral, P. L. Granja and M. A. Barbosa, *J. Biomat. Sci.-Polym. E*., **16**, 1575 (2005).
[44] Y. H. Zhu, H. Li, Q. Zheng, J. Q. Xu and X. X. Li, *Langmuir*, **28**, 7843 (2012).
[45] S. Farris, J. H. Song and Q. R. Huang, *J. Agric. Food Chem*., **58**, 998 (2010).
[46] N. Nishat, S. A. Khan, R. Rasool and S. Parveen, *J. Inorg. Organomet. P*., **21**, 673 (2011).